Motion planning and localization approaches for mobile robot navigation in ITER

A. Vale*, F. Valente*, I. Ribeiro†, J. Ferreira* and R. Ventura†
* Instituto de Plasmas e Fusão Nuclear – Laboratório Associado
Instituto Superior Técnico – Universidade Técnica de Lisboa
† Laboratório de Robótica e Sistemas em Engenharia e Ciência – Laboratório Associado
Instituto Superior Técnico – Universidade Técnica de Lisboa

***Abstract*—The ITER (International Thermonuclear Experimental Reactor) aims to prove the viability of fusion power. During the maintenance, the transport operations has to be carried out by autonomous mobile robots. The very high weight of the loads to be transported, together with bullet-proof reliability requirements, make the deployment of such robots a challenging scientific and technological problem. The paper addresses the problems of motion planning and the localization of these robots. The motion planning is based on line guidance and free roaming approaches to optimize trajectories for a rhombic like vehicle. The localization system is based on a laser range finder network, where two methods for pose estimation are used (Extended Kalman Filtering and bootstrap Particle Filtering). Experimental results, both from simulation and from small prototype are presented, illustrating the described methods.**

I. Introduction

The demand for energy is a critical problem the human societies have to address in a near future. The problem rises from the fact that fossil fuels are finite resources and renewable energies alone will not be enough to meet the demand. In this context, the ITER (International Thermonuclear Experimental Reactor) project aims to prove the viability of fusion power as an alternative and safe energy source. ITER will be built in Cadarache, France.

The Tokamak Building (TB) of ITER (Fig. 1) is where the reactor will be installed. During nominal and maintenance operations, the human presence is forbidden due to the high levels of radiation, and therefore, remote handling (RH) systems will play an important role in the ITER project. In [1] and [2] there is a description of RH systems in ITER. One of such systems is the Cask and Plug Remote Handling System (CPRHS), a mobile vehicle responsible for RH operations of transportation of contaminated components and equipment between the TB and the Hot Cell Building (HCB). The largest CPRHS has dimensions 8.5m x 2.62m x 3.7m (length, width, height) and when fully loaded weights approximately 100T. The CPRHS is divided into three main components: the Cask, that contains the load, the Pallet, that supports the Cask and the Cask Transfer System (CTS). The CTS acts as a mobile robot, by driving the entire vehicle, or by moving independently from the other components. The CTS has a rhombic kinematic configuration, as described in [3] and depicted in Fig. 1. This configuration allows to control the velocity, V_i, and orientation, θ_i, of each wheel $i \in \{R, F\}$. Additionally it allows for both wheels to follow the same path, in this paper referred as line guidance, or for each wheel to follow a different path, referred as free roaming, thus providing an increased flexibility, when moving in the cluttered environments of the TB and HCB.

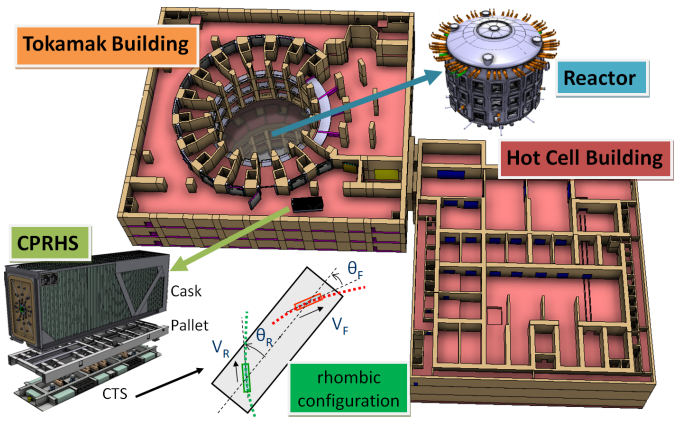

Fig. 1. Models of TB and HCB scenarios. Also displayed are detailed views of the reactor, of the CPRHS, and of the rhombic configuration.

To perform the required RH operations, the vehicle must move along optimized trajectories and for that purpose a motion planning framework described in previous works [4], [5], is used. This paper introduces two novelties: (1) the requirement that all trajectories are generated in order to maximize the part of the path that is shared by all the trajectories, and (2) experimental results of the approach in a 1:25 scale model real robot with rhombic kinematics.

A problem that is also addressed, in this paper, is the localization of the vehicle, by using a network of laser sensors placed in the scenario, along the lines presented in [6]. For testing purposes of the localization framework, a prototype of the CPRHS was built.

The paper is organized as follows: Section II presents the motion planning methodologies, Section III introduces the localization methods, Section IV presents the obtained results and in Section VI the conclusions and open issues are discussed.

II. Motion Planning

The vehicle is required to move along a path that simultaneously maximizes the clearance and minimizes the distance

between the start and the goal poses (position and orientation). Two motion planning methodologies, line guidance and free roaming, were developed.

A. Line guidance

The line guidance motion planning requires that both wheels of the vehicle follow the same path and, if adopted in ITER, the CTS will act as an Automated Guided Vehicle (AGV). This methodology is achieved in three main steps, [4], shown in Fig. 2: (1) geometric path evaluation, (2) path optimization, and (3) trajectory evaluation.

(1) Given the start and goal points, the map (a 2D projection at floor level of the scenario's 3D model, consisting in a set of line segments that defines walls and other obstacles) is decomposed into a set of triangles, by using Constrained Delaunay Triangulation, [7], to account for all walls. Then, the algorithm finds all sets of sequence of triangles that contain and link the start and goal points. Each sequence of triangles is converted into a sequence of points (mid point of the common edge of two consecutive triangles) yielding a path, shown in top left of Fig. 2. The shortest path is chosen as the geometric path.

(2) The initial geometric path does not guarantee a collision free path for a rigid body, with dimensions, and the path is not smooth (top center of Fig. 2). The optimization phase is a trade off between two criteria: clearance from obstacles, by increasing the distance from the vehicle to walls, and path smoothness, that results in shorter and smoother paths. The optimization procedure uses the elastic band concept, [8], where the path is modelled as an elastic band, similar to a series of connected springs subject to two types of forces: internal and external forces. The first are the internal elastic forces, whose magnitude is proportional to the amplitude of displacement and determine that the path becomes shorter. The repulsive forces are responsible for keeping the path, and thus the vehicle, away from the obstacles.

(3) The final trajectory is obtained by defining the velocity of the vehicle at each point of the optimized path, shown in top right of Fig. 2. In order to reduce the risk of collision in the case of a major malfunction, the velocity is reduced once the distance to the nearest obstacle decreases below a threshold value.

There are particular situations where given the above approach it is not possible to obtain a feasible solution, as illustrated in Fig. 3 - Left, where a clash occurs. By considering maneuvers in the motion planning procedure, it is possible to overcome this problem in these particular situations. A maneuver exists when the vehicle stops and changes its motion direction, in order to achieve a specified orientation, as illustrated in Fig. 3 - Right. A maneuver requires splitting the path in two sub-paths with the constrain that the final pose of the first sub-path is the initial pose of the next sub-path. Multiple maneuvers can be considered, with the path optimization being applied to each sub path. The point(s) of maneuver are introduced manually and its position can be set to be fixed or adjusted during optimization.

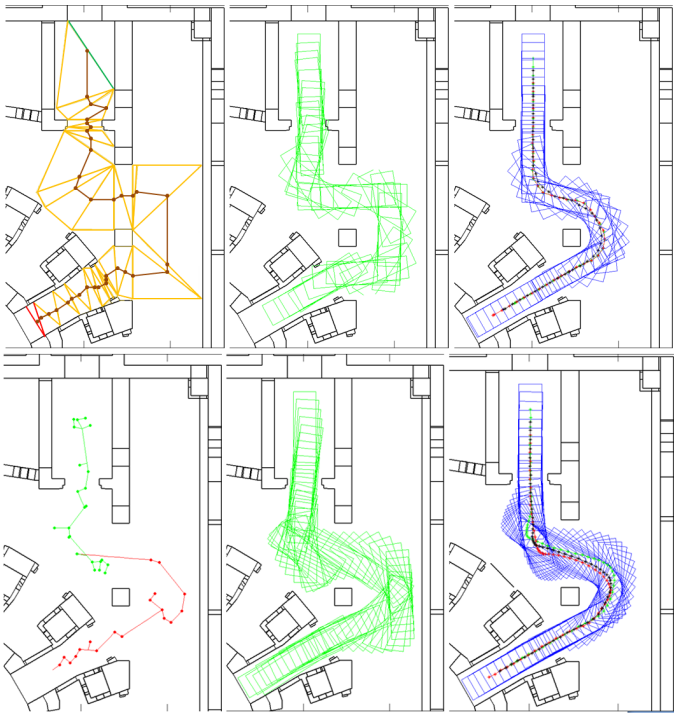

Fig. 2. Top (from left to right) - geometric path, poses over the geometric path and final optimized path shared by both wheels; Bottom (from left to right) - search for initial path by RRT, poses over the initial path and final optimized path with each wheel following its own path.

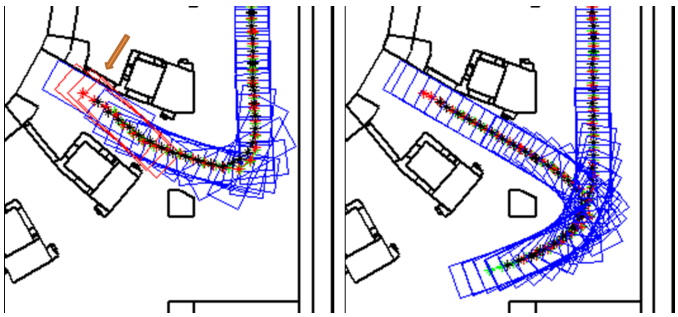

Fig. 3. Left - path shared by both wheels of the vehicle, with collision; Right - path with each wheel following its own path, without collision.

B. Free roaming

The free roaming motion planning does not constrain both wheels to the same path and each wheel can follow a different path. This methodology draws inspiration from the elastic band concept, [8], and was proposed in [5]. The vehicle's poses along the path act as rigid bodies, connected through internal interactions and subjected to external repulsive forces, resulting from the closest obstacles.

The initial path is given by the Rapidly-Exploring Random Tree (RRT), [9], which provides a collision free sequence of poses between a start and goal poses. The initial path, however, does not guarantee the maximization of clearance to obstacles nor path smoothness. The optimization procedure works then as a post processing method, that improves the quality of the initial path. Each pose is treated as a rigid body,

subjected to two types of forces: internal forces and external forces. The internal forces are the elastic force and torsional torque, originated from the virtual elastic and torsional springs, responsible for keeping consecutive poses connected and thus guaranteeing path smoothness. The external forces are the repulsive forces and torques that act on the rigid body (the vehicle's pose), resulting from obstacle proximity.

The final trajectory is generated by defining the velocity as a function of the minimum distance to obstacles, as described in section II-A. This motion planning methodology allows to fully explore the flexibility of the rhombic configuration, since the wheels are not constrained to follow the same path. In Fig. 4, it is shown an example where this methodology finds a solution that does not exist with the previous approach [1].

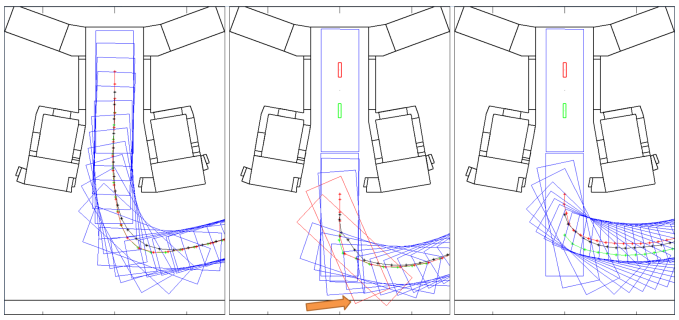

Fig. 4. Left - path shared by both wheels for a vehicle entering a port cell in TB, Center - path shared by both wheels, with collision, for a second vehicle entering the same port cell; Right - solution without collision with each wheel of the second vehicle following its own path.

C. Maximization of the common path of different paths

Given a set of paths that share the same starting pose, but differ on the arriving location, it becomes apparent that in terms of minimizing the areas accessed by the vehicle, it is logic, and required in ITER, to maximize the part of each path that is common to all paths. This leads to the definition of a common path, that is shared by all optimized paths, as shown in Fig. 5, where the common path starts in the lift area, covers a circular area around the reactor and returning to the lift. When a new path is generated, only the part that differs from the common path is optimized. This is performed by finding the nearest point on the common path, to the goal point. Usually, this nearest point is not the best starting condition for the path optimization, because it may require for the vehicle to make a sharp turn. A user defined threshold sets how further back from this nearest point the splitting point is defined (Fig. 5 - Right). When the start and goal configurations are defined, the optimization procedure can begin with either of the approaches described in II-A or II-B.

III. Localization

The localization problem consists in the estimation of the real pose relative to a global reference frame. During RH operations in ITER, the main radiation source will be the vehicle load, which means that on board sensors have a long and intense exposure which can shorten their lifetime. To overcome this constraint, it is proposed to install the sensors for vehicle localization on the building walls, reducing the exposure to radiation. This poses the challenge of where to place the sensors in the scenario and of how to perform the localization. Laser Range Finders (LRF) were adopted as sensors, since they are accurate and can be well shielded from radiation. The integration of a network with several sensors is necessary to cover all possible vehicle positions.

[1]It is here assumed without proof that if the optimized path found by one of the presented algorithms incurs in a clash, then there is no feasible solution under the given constraints.

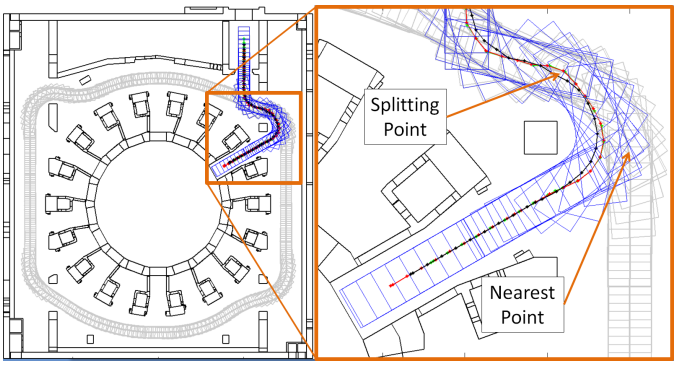

Fig. 5. Left - common path in TB depicted in grey; Right - detail view of an optimized path between the splitting point and the final point.

A. Sensor Network Optimization

A LRF sensor network is composed by several sensors, each one with the possibility of having a different parameterization. Sensor position and orientation are variable parameters chosen in the optimization process. Sensor field of view, angular resolution and standard deviation for distance measurement errors are fixed parameters that depend on the equipment. The optimization, herein described, maximizes, for a given number of sensors, the area obtained by the union of several visibility polygons, returning the sensor network parameterization with maximum coverage. An example LRF sensor network, with two sensors, is shown in Fig. 6 with visibility polygons for the respective sensors. The benefit of adding one more sensor to a network decreases as the number of sensors already present increases, [6]. The number of sensors to install is not optimized, it is picked based on a cost-benefit analysis of adding an extra sensor.

B. Bayesian approaches for Localization

Localization systems, with the framework presented in Fig. 6, give an estimation of vehicle pose integrating the measurements coming from the previously optimized LRF sensor network and the vehicle odometry.

Acquired measurements are distances from the corresponding LRF sensor to the nearest obstacle, in each direction. These directions depend only on sensor angular resolution and on the field of view. For each measurement acquisition, the directions are considered fixed and only the distances differ according to the surrounding obstacles.

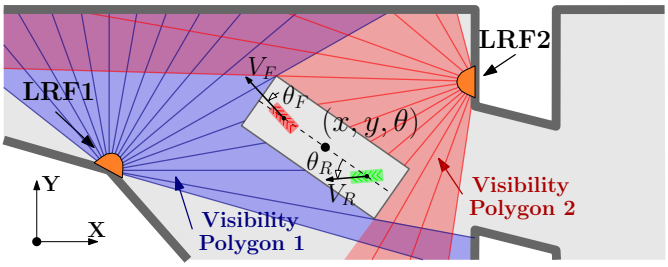

Fig. 6. Sensor Network and Localization system framework.

The two localization methods presented in this paper are standard Bayesian approaches, the Extended Kalman Filter (EKF), and bootstrap Particle Filter (PF) **??**, with new observation models, developed for this framework. The observation models are the main innovative contribution and this section is focused on its understanding.

1) Extended Kalman Filter: EKF uses a Jacobian matrix to relate the errors between the real and predicted measurements given estimated pose (innovation). There are four sets of measurements: i) the ones hitting the vehicle in real pose, ii) hitting the vehicle in predicted pose, iii) not hitting the vehicle in real pose, iv) not hitting the vehicle in predicted pose. A measurement is integrated by EKF only if it belongs to both i) and ii). This means that not all measurements can be integrated, only the ones that hit the vehicle. The residuals corresponding to measurements hitting the scenario walls have a Jacobian entrance equal to zero, because the distance measured to the wall do not depend directly on vehicle pose. This fact forces the method to neglect some information. Moreover, if the prediction is too far from reality, EKF does not integrate any measurement.

EKF predicted pose must be always near the real pose, otherwise the update step of EKF is ineffective. To overcome this problem, the number of measurements integrated on each iteration, is monitored, and, every time it drops below a certain threshold, EKF is restarted. It is possible to get a position estimation, for the restarting iteration, transforming measurements hitting the vehicle into Cartesian points and doing his mass center. The initial belief given for the restarting iteration of EKF has this mass center position, a random orientation and a high uncertainty. As the position is close to real one, the estimation converges to the real and uncertainty reduces.

The restarting step enables the global localization on the scenario, something that is not possible, using EKF, with onboard sensors.

2) Particle Filter: PF uses a set of particles to represent hypothetic poses of the vehicle. For each one of these poses, the observation model compares the predicted measurements with the real ones, assigning a likelihood to the respective particle.

It is possible, with this approach, to integrate all measurements from the network, and to adapt the observation model to the framework.

Observation model is a likelihood function that assumes measurements independent but not identically distributed. It distinguish two different distributions if the predicted measurements hit the hypothetic vehicle or not.

Let $\mathcal{N}(\mu, \sigma^2)$, be a normal distribution with μ mean and σ^2 variance. σ^2 is the variance assumed for the measurements, always greater then real measurement variance. $\mathcal{U}(a, b)$ is an uniform distribution with limits a and b.

For each measurement, the distribution is,

i) If it hits the vehicle, a linear mixture of:
   - $\mathcal{N}(d, \sigma^2)$, modeling measurements that hit the vehicle also in reality;
   - $\mathcal{N}(D, \sigma^2)$, modeling measurements that hit the walls in reality;
   - $\mathcal{U}(0, range)$, modeling outliers.

   The weight of $\mathcal{N}(d, \sigma^2)$ should always be greater then the others to reinforce the particles with correct prediction.

ii) If it hits the walls, a linear mixture of:
   - $\mathcal{N}(D, \sigma^2)$, modeling measurements that hit the walls also in reality;
   - $\mathcal{U}(0, D)$, modeling measurements that hit the vehicle in reality;
   - $\mathcal{U}(0, range)$, modeling outliers.

   The weight of $\mathcal{N}(D, \sigma^2)$ should be the highest to ensure that correct predictions have greater likelihood.

Being d the predicted distance to the vehicle, D the known distance to the nearest wall and $range$ the maximum range of the sensor. PF have the possibility for global localization, using the same principle used for EKF. When the measurement likelihood drops abruptly, the probability of generating particles around the measurement mass center rises, and, as PF can represent multi-modal distributions, a new mode starts to appear on this mass center. After some resample steps, all particles migrate near the correct pose of the vehicle and the likelihood rises again. The situation is similar to kidnapped mobile vehicle, but, with a global network of sensors, an approximation of the real pose, the measurement mass center, is easily discovered.

IV. Simulated Results

The simulation results were obtained with a software application tool developed in MATLAB environment: the Trajectory Evaluator and Simulator (TES), as illustrated in Fig. 7. The TES was developed not only to generate trajectories for ITER scenarios, but also to generate trajectories in a general map. The TES has a diversity of features that, besides trajectory generation, allow to do reports with information on the minimum distances to obstacles along the trajectories, as well as the location of the critical points in the scenario, to assess the risk of collision. It provides the area spanned by the vehicle along the path and it provides the option to export this information as a 3D CAD model to a CAD software, such as CATIA. Besides trajectories, TES can also simulate a basic guidance and localization system for the vehicle, controlling it along a given trajectory and giving a pose estimation based on simulated noisy LRF measurements.

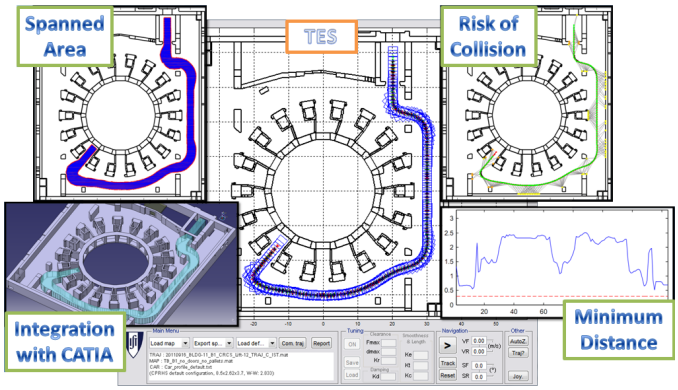

Fig. 7. TES main window and features.

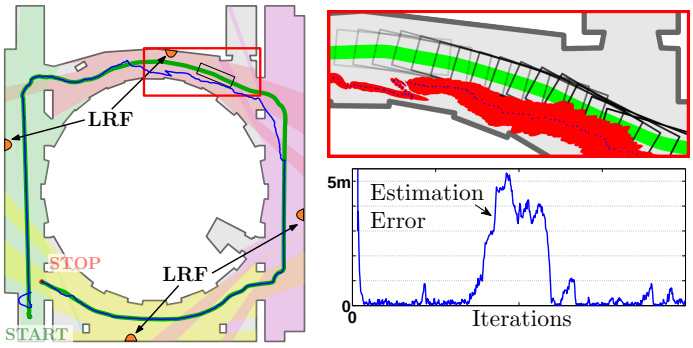

Fig. 9. Real trajectory (green) EKF estimated trajectory (blue) (left), Zoom box with estimated positions (blue) and certainty ellipses (red) (top right), Position error along the path (bottom right)

A. Optimized Trajectories

In TB, the CPRHS is required to dock in predefined locations during nominal operations. However, if a malfunction occurs during docking, trajectories for rescue missions were also required, where a CPRHS has to provide assistance to an already docked CPRHS (e.g., Fig. 3 Center and Right). In Fig. 8, optimized paths for docking and the corresponding optimized rescue paths are shown for one of the floors of TB. A total of 232 trajectories were computed in TB. The HCB is where the CPRHS is required to dock for loading/unloading operations and where parking areas for the vehicle are provided. On the right side of Fig. 8 it is shown optimized parking paths for one of the levels of HCB. A total of 304 trajectories were generated in HCB.

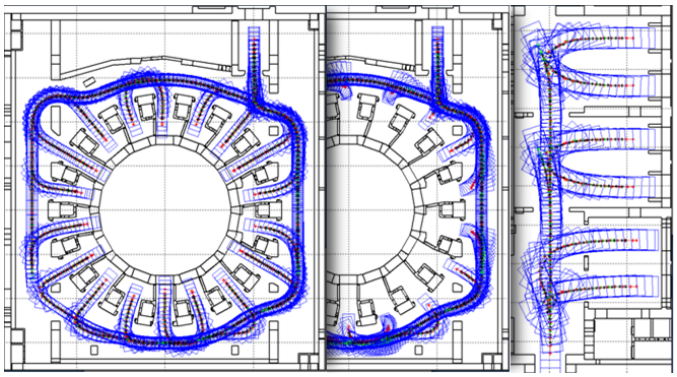

Fig. 8. Left - optimized paths for rescue missions of the CPRHS in TB; center - optimized paths for docking missions of the CPRHS in TB; right - optimized paths for parking missions of CPRHS in HCB.

B. Localization

The two localization approaches were implemented and compared in TES. The simulation results, consider a network of 4 sensors, with angular resolution of 1^o and standard deviation for distance measurement of $10cm$. Both approaches can localize the vehicle correctly due to the adopted observation models. EKF performance, in Fig. 9, presents some limitations in accuracy and robustness but it has a very interesting computation performance. In particular situations, like the one highlighted in Fig. 9 (top right), EKF loses stability and the estimation error becomes very high. Red ellipses show that EKF estimation has an unacceptable high uncertainty, facing the tight safety margins inside ITER.

PF performance, in Fig. 10, presents very reliable results, it is very accurate and robust to all situations tested in ITER scenarios. The results show very small uncertainty, shown by the small red ellipses in Fig. 10 (top right), low estimation errors, and no losses of stability. PF downside is the high computation effort required, it is 30 times slower then EKF for the sensor network used on this simulation. PF integrates all measurements while EKF takes only the ones hitting the vehicle. Position estimation errors, for EKF and PF, along the trajectory, are presented on Fig. 9 and Fig. 10 (bottom right), respectively. Both approaches are initialized with random estimation, explaining the high estimation error in the beginning. Both approaches are able to converge from this random pose due to the global localization feature explained on previous section. Comparing both approaches, EKF estimation error is unacceptable for an ITER application while PF present very reliable results. On this simulation, mean position estimation error for EKF is $0.9m$ while for PF it is $0.06m$. Maximum estimation error, after global localization, is $5.3m$ for EKF and for PF is $0.19m$. From these two localization approaches, PF is the most appropriate for application with this framework. EKF performance rises with the number of sensors installed on the scenario. With many sensors it is guaranteed that EKF always integrate many measurements becoming more accurate. PF becomes more accurate with more sensors, but with very high computation cost.

V. Experimental Results

The experimental setup, shown in Fig. 11 (left), includes a single Hokuyo LRF sensor and a CPRHS prototype built in LEGO Mindstorms. The LRF sensor has a field of view of 240^o and angular resolution of 0.36^o. The prototype, with a 1:25 scale, describes a simple trajectory in a rectangular map without obstacles. For simplicity, the described trajectory is not a result from optimization, it is the result from simple commands sent directly from operator to the vehicle.

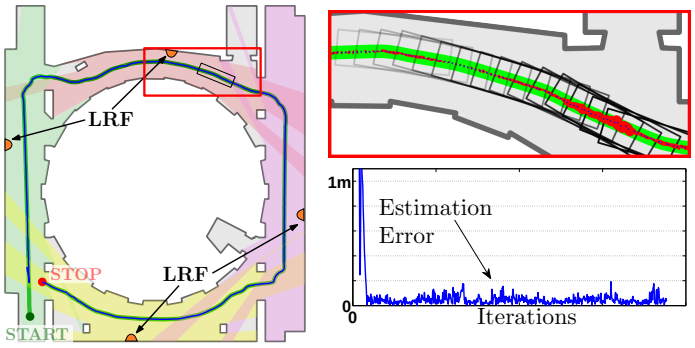

Fig. 10. Real trajectory (green) PF estimated trajectory (blue) (left), Zoom box with estimated positions (blue) and certainty ellipses (red) (top right), Position error along the path (bottom right)

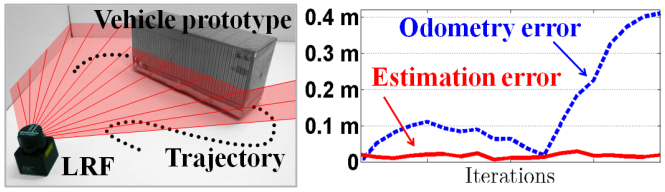

Fig. 11. Experimental framework (left), Error along trajectory (right)

Way points along the trajectory were manually registered and compared with the ones estimated by the localization system (Fig. 12). The position estimation error, presented in the plot of Fig. 11 (right), is below 0.3cm and the orientation error is less then 8^o. The results are biased by the erroneous odometry, due to prototype encoder resolution and wheel slippage. The error between real position and integrated position, given the vehicle odometry, is also shown in Fig. 11 (right).

The estimations, for this experiment, were computed offline. The data acquisition rate was $5Hz$, but PF mean computation rate, with 300 particle, was $4Hz$. The PF approach achieves good results, even with a highly erroneous odometry, the main problem for a real time implementation is the computational effort required.

VI. Conclusions and Open Issues

For the generation of the optimized paths, the two proposed path planning methodologies were used. The majority of the trajectories are feasible with the line guidance approach, incorporating maneuvers whenever necessary. The free roaming approach is of great importance in rescue situations, where the flexibility of the rhombic configuration is explored to compute feasible paths, where the line guidance method fails.

The implemented localization methods, EKF and PF, using a sensor network of LRF outside of the vehicle, were able to locate the vehicle in a simulated environment. The PF method proved to more reliable than the EKF, even in the case of sensor failure, however, the performance is highly dependent of the total coverage by the sensor network.

Further work is required to evaluate the performance of the localization methods in terms of sensor redundancy and compare the localization results between line guidance and free roaming trajectories. Control methods in real time that take into consideration the experimental localization results, should also be addressed.

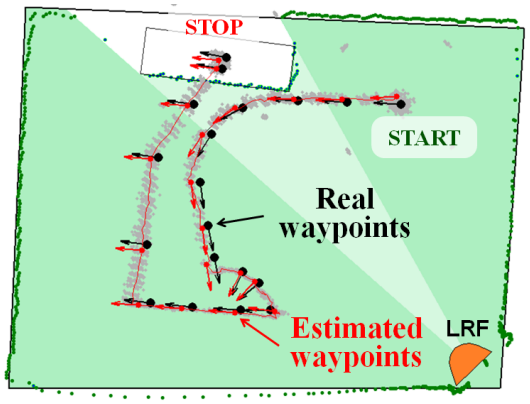

Fig. 12. Experimental trajectory with real vehicle poses (black) and Estimated poses (red)

Acknowledgment

The work was supported by the grants F4E-2008-GRT-016 (MS-RH) and F4E-GRT-276-01 (MS-RH) funded by the European Joint Undertaking for ITER and the Development of Fusion for Energy (F4E) and by FCT in the frame of the Contract of Associate Laboratories of Instituto de Plasmas e Fusão Nuclear/IST and Laboratório de Robótica e Sistemas em Engenharia e Ciências/IST (PEst-OE/EEI/LA0009/2011). The views expressed in this publication are the sole responsibility of the authors. F4E is not liable for the use which might be made of the information in this publication.

References

[1] I. Ribeiro, C. Damiani, A. Tesini, S. Kakudate, M. Siuko and C. Neri, *The Remote Handling Systems for ITER*, Fusion Engineering and Design, vol. 86, pp. 471-477, 2011.

[2] C. Gonzlez, C. Damiani, J-P. Friconneau, A. Tesini, I. Ribeiro and A. Vale, *ITER Transfer Cask System: status of design, issues and future development.*, Fusion Engineering and Design, vol. 85, pp. 2295-2299, 2010.

[3] I. Ribeiro, P. Lima and R. Ferreira, *Conceptual Study on Flexible Guidance and Navigation for ITER Remote Handling Transport Casks*, Proc. of the 17th IEEE/NPSS Symp. on Fusion Engineering, pp. 969-972, San Diego, USA 1995.

[4] D. Fonte, F. Valente, A. Vale and I. Ribeiro, *A motion planning methodology for rhombic-like vehicles for ITER remote handling operations*, 7th Symp. on Intelligent Autonomous Vehicles, Italy, 2010.

[5] D. Fonte, F. Valente, A. Vale and I. Ribeiro, *Path Optimization of Rhombic-Like Vehicles: An Approach Based on Rigid Body Dynamic*, Proc. of the 15th IEEE International Conf. on Advanced Robotics, pp. 106-111, Tallin, Estonia 2011.

[6] J. Ferreira, A. Vale and R. Ventura, *Optimizing range finder sensor network coverage in Indoor Environment*, 7th Symp. on Intelligent Autonomous Vehicles, Italy, 2010.

[7] L. P. Chew, *Constrained Delaunay Triangulations*, Proc. of the Third Annual Symp. on Computational Geometry, pp 215-222, Waterloo, Ontario, Canada, 1987.

[8] S. Quinlan and O. Khatib, *Elastic Bands: Connecting Path Planning and Control*, Proc. IEEE Conference Robotics and Automation, vol. 2, pp 802-807, Atlanta, USA, 1993.

[9] S. M. La Valle and J. J. Kuffner, *Rapidly-exploring random trees: Progress and prospects*,In B. R. Donald, K. M. Lynch and D. Rus, editors, Algorithmic and Computational Robotics: New Directions, pp 293-308, A K Peters, Wellesley, MA, 2001.

[10] J.S. Gutmann, W. Burgard, D. Fox, and K. Konolige, *An experimental comparison of localization methods*, Proc. of the IEEE/RSJ International Conference, pp. 736–743, IEEE, 2002.